

of discussion seems first to have been introduced by Donnay & Donnay (1959). Their use in the same connexion was also suggested by Landau & Lifshitz (1958).

### References

- ABRAMAM, A. (1961). *The Principles of Nuclear Magnetism*. London: Oxford Univ. Press.
- AU, R., COWEN, J. A., SPENCE, R. D. & VAN TILL, H. (1965). *Low Temperature Physics* p. 877. New York: Plenum Press.
- DONNAY, J. D. H. & DONNAY, G. (1959). *C.r. Acad. Sci. Paris*, **248**, 3317.
- HEESCH, H. (1930). *Z. Kristallogr.* **73**, 325.
- KOPTSIK, V. A. (1966). *Shubnikov Groups*. Moscow Univ. Press.
- LANDAU, L. & LIFSHITZ, E. (1958). *Statistical Physics*. London: Pergamon Press.
- LOMONT, J. S. (1959). *Applications of Finite Groups*. New York: Academic Press.
- NYE, J. F. (1957). *Physical Properties of Crystals*. Oxford: Clarendon Press.
- OPECHOWSKI, W. & GUCCIONE, R. (1965). *Magnetism*. Vol. II A. Edited by G. T. RADO & H. SUHL. p. 105. New York: Academic Press.
- RIEDEL, E. P. & SPENCE, R. D. (1960). *Physica*, **26**, 1174.
- SPENCE, R. D. & NAGARAJAN, V. (1966). *Phys. Rev.* **149**, 191

*Acta Cryst.* (1968). **A24**, 497

## The Influence of Thermal Parameters on Electron Density Maps

BY ROBERT F. STEWART

*Mellon Institute, 4400 Fifth Avenue, Pittsburgh, Pennsylvania 15213, U.S.A.*

(Received 24 November 1967 and in revised form 30 January 1968)

Accurate formulae for the convolution of atomic one-electron density functions onto anisotropic Gaussian distribution functions are presented. Theoretical time average electron density functions for some first row atoms at various degrees of resolution are analyzed by variation of Debye-Waller factors. The calculations show that for present day precision in thermal parameters Fourier difference maps suffer an unmanageable bias near the time-average nuclear positions. Residual densities at distances greater than 0.4 Å from time-average nuclear positions are affected only marginally by errors in atomic thermal parameters. The upper limit in  $\sin \theta/\lambda$  for proper reconstruction of valence densities is also studied. For the room temperature case, 0.8 Å<sup>-1</sup> in  $\sin \theta/\lambda$  is adequate; for low temperature work ( $\sim -180^\circ\text{C}$ ) 1.2 Å<sup>-1</sup> is more appropriate.

### Introduction

Electron density maps evaluated by Fourier syntheses using X-ray diffraction structure factors,  $F_o$ 's, can present a variety of distortions as a result of experimental limitations. In the difference Fourier technique, parametric errors in the calculated structure factors,  $F_c$ 's, must also be considered. A recent study on bonded electron distributions in organic molecular crystals (O'Connell, Rae & Maslen, 1966) has prompted the author to investigate some errors inherent in the difference Fourier syntheses of X-ray diffraction data. It is important that these effects be reviewed and studied in quantitative detail, so that one can make meaningful interpretations of electron density maps. In the present paper we shall assume that there is an adequate macroscopic theory for the determination of structure factors from X-ray diffraction intensities of real crystals (*cf.* Zachariasen, 1967). We shall also assume that the observed structure factors can be phased by conventional structure factor calculations (this restricts us primarily to centric structures). We will thus confine ourselves to the problems of series termination error

and parametric errors in the difference Fourier synthesis technique.

If, in a Fourier difference synthesis, only the (1s)<sup>2</sup> density is subtracted out, we shall call the residual density a valence electron density map. For a molecular crystal, comprised of first row atoms, such a density map should be of interest to chemists and is hopefully interpretable in terms of 2s and 2p orbital product density functions. The influence of thermal motion on electron densities is an important effect to be considered.

In an analysis of the valence electron density  $\varrho_v$ , however, the error must be assessed from the corresponding errors in  $\bar{\rho}_o$  and  $\bar{\rho}_c$ , the respective incomplete Fourier series of the observed and calculated structure factors. Thus

$$\Delta F_v = F_o - F_c$$

implies

$$\varrho_v = \bar{\rho}_o - \bar{\rho}_c$$

and any variation in  $\varrho_v$  is

$$\delta \varrho_v = \delta \bar{\rho}_o - \delta \bar{\rho}_c .$$

The vibrational modification in the one-electron density of a carbon atom has been studied in detail (Higgs, 1953). Higgs's work was further developed by Atoji (1957) by extension to all first row atoms as well as some heavier atoms. Ibers (1961) has also studied carbon atom electron density peak shapes as a function of both the Debye-Waller factor and of the limiting X-ray sphere radius in  $\sin \theta/\lambda$ . Allmann (1967) has studied the same problem for the  $K$  shell and  $L$  shell density functions of the carbon atom.

In the present work the emphasis is on the orbital product contribution to the total density for some first row atoms. The influence of thermal averaging of each orbital product contribution and its variation with the Debye-Waller factor is studied. The effect of series termination on the Fourier synthesis representation of each contribution has also been analyzed. Throughout these calculations SCF wavefunctions of high accuracy are utilized. The effects of atomic position errors will not be treated here. They have been investigated by Dawson (1964). We will confine our attention to parametric errors in  $\bar{\rho}_c$  and assume that

the observed structure factors are sufficiently accurate to set  $\delta\bar{\rho}_o=0$ . In particular, we want to analyze the variation in  $\varrho_v$  as a function of variation in the Debye-Waller factor (or corresponding anisotropic thermal parameters) introduced into the  $F_c$  calculation. For simplicity, harmonic motion for the atoms is assumed throughout. To the degree that anharmonicities are important, some conclusions in this paper may have to be modified.

#### Time average electron densities

A harmonic oscillator in thermal equilibrium with its environment has a Gaussian distribution function (Bloch, 1932). In the adiabatic approximation, the time average one-electron density of an atom will be the convolution of the stationary atomic density onto the nuclear distribution function (Higgs, 1953).

$$\bar{\rho}(\mathbf{r}) = \int_{\mathbf{u}} \varrho(\mathbf{r}-\mathbf{u})g(\mathbf{u})d\mathbf{u} \quad (1)$$

where

$$g(\mathbf{u}) = \{||\beta||/(2\pi)^3\}^{1/2} \exp(-\frac{1}{2}\mathbf{u}^T\beta\mathbf{u})$$

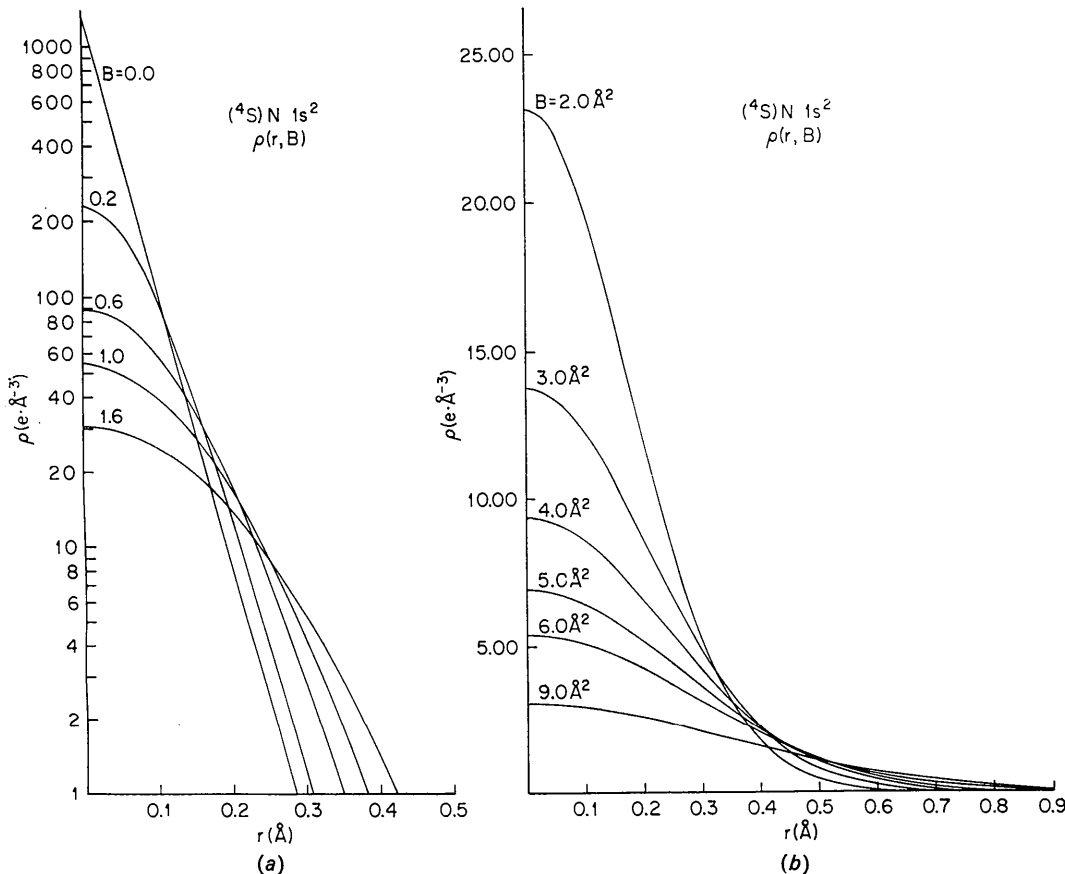


Fig. 1. Atomic 1s densities of  $(^4S)$  N atom as a function of distance from the time-average nuclear position for several Debye-Waller factors. The corresponding root mean square amplitude of vibration,  $\langle u^2 \rangle^{1/2} = [3B/8\pi^2]^{1/2}$ . The density functions are normalized so that  $4\pi \int_0^\infty r^2 \varrho(r, B) dr = 2$  electrons. (a) The density is represented on a logarithmic scale. (b) The ordinate is on a linear scale. The range of  $B$  values is the usual room temperature case for organic molecular crystals.

( $\mathbf{u}$  is a column vector and  $\mathbf{u}^t$  is a row vector) and

$$\text{tr } (\beta^{-1}) = \langle \mathbf{u}^t \mathbf{u} \rangle_{\text{av}}.$$

The tensor,  $\beta$ , is symmetric, real, positive definite, and thus can be diagonalized. From analytical atomic orbitals built up of Slater type orbitals (STO's), the time average one-electron density function can be represented analytically with parabolic cylinder functions (Atoji, 1957). The more general problem of anisotropic thermal motion for non-spherical atomic densities is rather intractable for the radial STO's. An adequate basis set for the problem here is one made up of Gaussian type orbitals (GTO's). The self-consistent field atomic orbitals, made up of a linear combination of GTO's, obtained by Huzinaga (1965) can be compared to Clementi's STO results (Clementi, Roothaan & Yoshimine, 1962). The one-electron density functions from the corresponding SCF wave functions are in agreement to better than 1% everywhere. At the nucleus there is the largest discrepancy. In particular the 1s orbital product contribution to the density yields the greatest difference (*e.g.* for  $(^4S)$  N, the STO 1s<sup>2</sup> result is 1326 e. $\text{\AA}^{-3}$  at the nucleus and the corresponding GTO is 1313 e. $\text{\AA}^{-3}$ ). Moreover, the corresponding STO and GTO scattering factors for all the first row atoms

are in agreement to four decimal places up to  $\sin \theta / \lambda = 2.00 \text{\AA}^{-1}$ . For an X-ray scattering analysis, Huzinaga's GTO's are sufficient for an electron density study.

From Huzinaga's basis functions for the 1s and 2s AO's the time average density (1) for anisotropic nuclear motion, where the vector  $\mathbf{r}$  has Cartesian components along the principal axes of  $\beta$ , is

$$\begin{aligned} \rho_{ns}(\mathbf{r}, \beta) = & \frac{N}{(a_0)^3} \left( \frac{2}{\pi} \right)^{3/2} \sum_{p,q} C_p C_q \\ & \times \zeta_p^{3/4} \zeta_q^{3/4} \exp \left[ -(\zeta_p + \zeta_q) \left( \frac{X^2}{\alpha_x} + \frac{Y^2}{\alpha_y} + \frac{Z^2}{\alpha_z} \right) \right], \quad (2) \end{aligned}$$

where

$$\alpha_x = 4\beta_x(\zeta_p + \zeta_q) + 1$$

$$\beta_x = B_x/(4\pi a_0)^2 = U_x/2a_0^2.$$

$U_x$  is the mean square amplitude ( $\text{\AA}^2$ ) of vibration in the  $x$  direction.  $a_0$  is the Bohr radius ( $0.529167 \text{\AA}$ ). The  $C_p$  and  $\zeta_p$  are the coefficients appropriate to the particular atomic orbital and the sum is over the basis functions. For the ten GTO basis functions reported by Huzinaga (1965), the density functions (2) for each 1s and 2s orbital product are series of fifty-five Gaussians.  $N$  is the number of electrons in the atomic orbital.

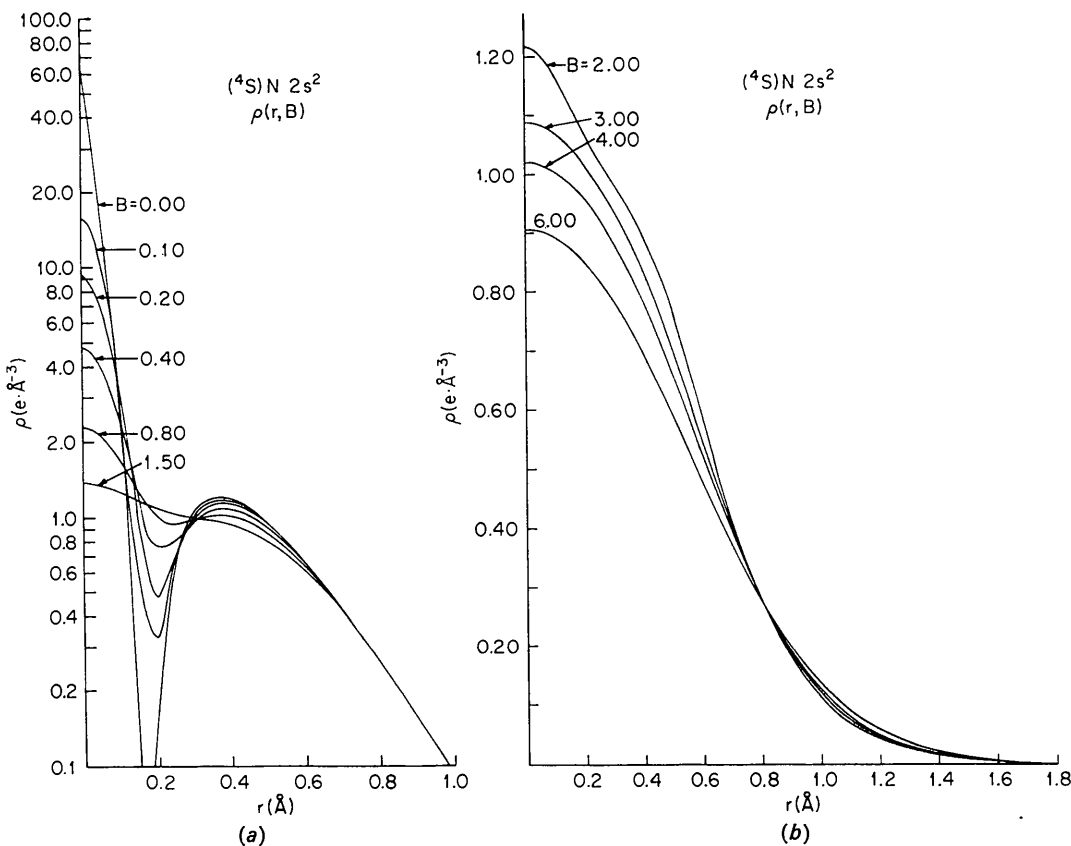


Fig. 2. Vibrational modification of the atomic 2s density piece for  $(^4S)$  N atom. The density functions are normalized as in Fig. 1 to 2 electrons. (a) The density is represented on a logarithmic scale. (b) The ordinate is on a linear scale.

The spherically averaged  $2p$  density convoluted onto anisotropic nuclear motion is

$$\begin{aligned} \varrho_{2p}(\mathbf{r}, \beta) = & \frac{4N}{3(a_0)^3} \left( \frac{2}{\pi} \right)^{3/2} \sum_{p,q} C_p C_q \\ & \times \frac{\zeta_p^{5/4} \zeta_q^{5/4}}{\alpha_x^{1/2} \alpha_y^{1/2} \alpha_z^{1/2}} \exp [\arg] [(2\beta_x + X^2/\alpha_x)/\alpha_x \\ & + (2\beta_y + Y^2/\alpha_y)/\alpha_y + (2\beta_z + Z^2/\alpha_z)/\alpha_z], \quad (3) \end{aligned}$$

where

$$\arg = -(\zeta_p + \zeta_q) (X^2/\alpha_x + Y^2/\alpha_y + Z^2/\alpha_z).$$

For the  $2p$  atomic orbital, there are six GTO's, so that (3) is a series of twenty-one terms. Expressions (2) and (3) allow us to formulate a good picture of the time average density for a vibrating atom. In a real X-ray diffraction experiment, however, we are limited to a finite set of structure factors and the restrictions

imposed by the limiting sphere for the reflections must be considered. In a Fourier difference synthesis, where a precalculated atomic scattering factor is subtracted out, the actual density removed for isotropic thermal motion is,

$$\begin{aligned} \varrho_{\text{at}}(r, S_0, B) \\ = [1/(2\pi^2)] \int_0^{S_0} S^2 f_{\text{at}}(S) j_0(Sr) \exp [-(4\pi)^{-2} BS^2] dS. \quad (4) \end{aligned}$$

$S_0$  is the limiting sphere radius,  $4\pi \sin \theta_{\max}/\lambda$ , when  $\theta_{\max}$  is the maximum Bragg angle for the observed data. The variable of integration,  $S$ , is  $4\pi \sin \theta/\lambda$ ;  $j_0(Sr)$  is a zero order spherical Bessel function;  $B$  is the usual Debye-Waller factor; and  $f_{\text{at}}(S)$  is the scattering factor for the atom or for some appropriate density function (e.g. the core electron orbital product) of a first row atom. Since accurate analytical SCF wavefunctions are available (Clementi, Roothaan &

Table 1. Partial derivative of the 1s density function for  ${}^4S$  of N atom with respect to  $B$ , the Debye-Waller factor  
The limits,  $\sin \theta_{\max}/\lambda$ , are in  $\text{\AA}^{-1}$ . The Debye-Waller factors are in  $\text{\AA}^2$  and the values of  $R$  are in  $\text{\AA}$ .

$R$	$B$	$\partial \varrho_{1s}(r, B, S_0)/\partial B$											
		Limit 0·65											
0	2·50	-1·964	-1·713	-1·498	-1·313	-1·154	-1·017	-0·899	-0·796	-0·707	-0·629	-0·562	-0·503
0·050	-1·928	-1·683	-1·472	-1·291	-1·135	-1·001	-0·884	-0·783	-0·696	-0·620	-0·554	-0·496	
0·100	-1·825	-1·594	-1·396	-1·225	-1·079	-0·952	-0·842	-0·747	-0·664	-0·592	-0·529	-0·475	
0·150	-1·660	-1·453	-1·275	-1·121	-0·989	-0·874	-0·775	-0·688	-0·613	-0·548	-0·491	-0·441	
0·200	-1·447	-1·270	-1·117	-0·985	-0·871	-0·773	-0·687	-0·612	-0·547	-0·490	-0·440	-0·396	
0·250	-1·200	-1·057	-0·934	-0·827	-0·735	-0·654	-0·584	-0·523	-0·469	-0·422	-0·380	-0·344	
0·300	-0·935	-0·829	-0·737	-0·657	-0·587	-0·526	-0·473	-0·426	-0·384	-0·348	-0·315	-0·287	
0·350	-0·670	-0·600	-0·539	-0·486	-0·438	-0·396	-0·360	-0·327	-0·298	-0·272	-0·248	-0·228	
0·400	-0·420	-0·384	-0·352	-0·322	-0·296	-0·272	-0·251	-0·231	-0·214	-0·198	-0·183	-0·170	
0·450	-0·199	-0·192	-0·184	-0·176	-0·168	-0·160	-0·152	-0·144	-0·137	-0·130	-0·123	-0·117	
0·500	-0·018	-0·033	-0·044	-0·053	-0·060	-0·064	-0·067	-0·069	-0·070	-0·071	-0·070	-0·069	
Limit 0·80													
0	1·50	-5·527	-4·499	-3·683	-3·032	-2·511	-2·092	-1·754	-1·479	-1·254	-1·071	-0·919	-0·793
0·050	-5·377	-4·380	-3·588	-2·956	-2·450	-2·043	-1·714	-1·446	-1·228	-1·049	-0·901	-0·778	
0·100	-4·942	-4·035	-3·313	-2·737	-2·274	-1·901	-1·599	-1·352	-1·151	-0·986	-0·849	-0·735	
0·150	-4·271	-3·502	-2·888	-2·397	-2·000	-1·680	-1·419	-1·206	-1·031	-0·886	-0·766	-0·666	
0·200	-3·433	-2·836	-2·356	-1·969	-1·656	-1·401	-1·192	-1·020	-0·878	-0·760	-0·661	-0·579	
0·250	-2·516	-2·104	-1·769	-1·497	-1·273	-1·089	-0·938	-0·811	-0·706	-0·617	-0·542	-0·479	
0·300	-1·608	-1·375	-1·182	-1·022	-0·887	-0·774	-0·678	-0·597	-0·528	-0·469	-0·418	-0·374	
0·350	-0·788	-0·714	-0·646	-0·584	-0·529	-0·479	-0·434	-0·394	-0·358	-0·326	-0·298	-0·272	
0·400	-0·120	-0·168	-0·199	-0·216	-0·224	-0·225	-0·222	-0·216	-0·208	-0·199	-0·189	-0·179	
0·450	0·359	0·230	0·133	0·062	0·011	-0·027	-0·054	-0·072	-0·085	-0·093	-0·097	-0·099	
0·500	0·638	0·470	0·342	0·243	0·167	0·110	0·066	0·032	0·007	-0·012	-0·026	-0·036	
Limit 1·20													
0	0·50	0·591	-24·987	-16·369	-11·055	-7·698	-5·521	-4·072	-3·082	-2·388	-1·889	-1·522	-1·246
0·050	-36·926	-23·575	-15·507	-10·516	-7·352	-5·294	-3·918	-2·975	-2·312	-1·833	-1·481	-1·215	
0·100	-30·404	-19·667	-13·113	-9·013	-6·385	-4·654	-3·484	-2·673	-2·096	-1·676	-1·363	-1·125	
0·150	-21·263	-14·149	-9·704	-6·855	-4·982	-3·719	-2·844	-2·223	-1·772	-1·437	-1·184	-0·988	
0·200	-11·545	-8·204	-5·978	-4·461	-3·403	-2·649	-2·101	-1·694	-1·386	-1·150	-0·965	-0·819	
0·250	-3·201	-2·977	-2·622	-2·250	-1·908	-1·613	-1·364	-1·158	-0·988	-0·848	-0·732	-0·636	
0·300	2·436	0·721	-0·137	-0·539	-0·704	-0·745	-0·726	-0·679	-0·622	-0·564	-0·508	-0·457	
0·350	4·938	2·589	1·264	0·518	0·102	-0·126	-0·244	-0·301	-0·322	-0·322	-0·312	-0·296	
0·400	4·761	2·832	1·661	0·945	0·503	0·231	0·063	-0·040	-0·101	-0·137	-0·155	-0·164	
0·450	2·955	2·012	1·355	0·899	0·583	0·364	0·214	0·110	0·039	-0·010	-0·042	-0·064	
0·500	0·733	0·813	0·732	0·600	0·465	0·346	0·248	0·170	0·110	0·065	0·030	0·005	

Yoshimine, 1962; Huzinaga, 1965), (4) can be accurately evaluated by numerical integration.

The extension of (4) to anisotropic thermal motion is,

$$\begin{aligned} \varrho(x, y, z, S_x^0, S_y^0, S_z^0, B_x, B_y, B_z) \\ = [1/(2\pi)^3] \int_{-S_x^0}^{S_x^0} \int_{-S_y^0}^{S_y^0} \int_{-S_z^0}^{S_z^0} f_{at}(S_x, S_y, S_z) \\ \times \exp [-(4\pi)^{-2}(B_x S_x^2 + B_y S_y^2 + B_z S_z^2)] \\ \times \cos(xS_x) \cos(yS_y) \cos(zS_z) dS_x dS_y dS_z. \quad (5) \end{aligned}$$

The limits of the integrations,  $(S_x^0, S_y^0, S_z^0)$ , are taken along the principal directions of the thermal ellipsoid. The three-dimensional integrals in (5) can also be accurately determined by numerical techniques; in fact, the scattering factors from Huzinaga's GTO-AO's enable the problem to be reduced to a product of one-dimensional integrals. One may use (5) and its approx-

priate partial derivatives for detailed analysis of density maps derived from X-ray diffraction data. For the sake of clarity, however, we will study the results of (4) and the partial derivatives of (4) with respect to  $B$  in this paper.

### Results and discussion

In the following discussion we will consider the results for the nitrogen atom in detail. The first row atoms, boron through fluorine, have been analyzed in a similar fashion, but will not be presented here. Nitrogen holds a middle position in most of the trends, and serves as an example for the other atoms. Detailed results for the other first row atoms may be easily obtained through the use of equations (2) through (5).

Fig. 1 displays a family of nitrogen ( ${}^4S$ ) core ( $1s^2$ ) electron density curves as a function of  $r$  for various Debye-Waller factors. These curves were computed

Table 2. Partial derivative of the total density for  ${}^4S$  of N atom with respect to  $B$

The units are the same as for Table 1.

$R$	$B$	$\frac{\partial \varrho(r, B, S_0)}{\partial B}$											
		Limit 0.65											
0	-2.259	-1.988	-1.754	-1.552	-1.377	-1.226	-1.094	-0.979	-0.879	-0.792	-0.715	-0.647	
0.050	-2.221	-1.955	-1.726	-1.528	-1.356	-1.207	-1.078	-0.965	-0.867	-0.781	-0.705	-0.639	
0.100	-2.109	-1.858	-1.642	-1.456	-1.294	-1.153	-1.031	-0.924	-0.831	-0.749	-0.678	-0.614	
0.150	-1.931	-1.705	-1.510	-1.341	-1.194	-1.067	-0.956	-0.859	-0.774	-0.699	-0.633	-0.575	
0.200	-1.700	-1.506	-1.338	-1.192	-1.065	-0.954	-0.857	-0.772	-0.698	-0.633	-0.575	-0.524	
0.250	-1.431	-1.273	-1.136	-1.017	-0.913	-0.821	-0.741	-0.671	-0.609	-0.554	-0.506	-0.463	
0.300	-1.141	-1.022	-0.919	-0.828	-0.748	-0.677	-0.615	-0.560	-0.512	-0.468	-0.430	-0.395	
0.350	-0.849	-0.769	-0.698	-0.635	-0.580	-0.530	-0.486	-0.447	-0.411	-0.380	-0.351	-0.325	
0.400	-0.572	-0.527	-0.487	-0.451	-0.418	-0.388	-0.361	-0.336	-0.313	-0.293	-0.274	-0.256	
0.450	-0.323	-0.310	-0.296	-0.283	-0.270	-0.257	-0.245	-0.233	-0.222	-0.211	-0.201	-0.191	
0.500	-0.115	-0.126	-0.134	-0.139	-0.142	-0.144	-0.144	-0.143	-0.141	-0.138	-0.135	-0.132	
Limit 0.80													
$R$	$B$	1.50	2.00	2.50	3.00	3.50	4.00	4.50	5.00	5.50	6.00	6.50	7.00
		-5.814	-4.774	-3.945	-3.282	-2.748	-2.316	-1.966	-1.679	-1.444	-1.249	-1.088	-0.953
0	-5.662	-4.653	-3.849	-3.204	-2.685	-2.266	-1.924	-1.645	-1.416	-1.226	-1.068	-0.937	
0.050	-5.223	-4.304	-3.569	-2.980	-2.504	-2.119	-1.804	-1.547	-1.335	-1.159	-1.012	-0.889	
0.100	-4.544	-3.762	-3.136	-2.631	-2.222	-1.889	-1.617	-1.393	-1.207	-1.053	-0.924	-0.815	
0.150	-3.695	-3.085	-2.592	-2.192	-1.866	-1.599	-1.379	-1.197	-1.045	-0.918	-0.811	-0.720	
0.200	-2.763	-2.337	-1.989	-1.704	-1.469	-1.274	-1.112	-0.976	-0.861	-0.764	-0.681	-0.610	
0.250	-1.835	-1.589	-1.384	-1.211	-1.066	-0.942	-0.837	-0.747	-0.670	-0.603	-0.545	-0.494	
0.300	-0.993	-0.905	-0.825	-0.753	-0.688	-0.629	-0.576	-0.528	-0.485	-0.446	-0.411	-0.380	
0.350	-0.298	-0.335	-0.355	-0.363	-0.362	-0.356	-0.345	-0.333	-0.319	-0.304	-0.289	-0.274	
0.400	0.210	0.091	0.003	-0.060	-0.106	-0.137	-0.158	-0.171	-0.179	-0.182	-0.183	-0.181	
0.450	0.520	0.360	0.237	0.144	0.074	0.020	-0.019	-0.049	-0.071	-0.086	-0.097	-0.104	
Limit 1.20													
$R$	$B$	0.50	1.00	1.50	2.00	2.50	3.00	3.50	4.00	4.50	5.00	5.50	6.00
		-39.559	-25.239	-16.615	-11.297	-7.935	-5.752	-4.296	-3.296	-2.593	-2.084	-1.708	-1.422
0	-37.191	-23.826	-15.752	-10.758	-7.589	-5.524	-4.141	-3.189	-2.516	-2.028	-1.665	-1.390	
0.050	-30.660	-19.916	-13.357	-9.253	-6.619	-4.881	-3.703	-2.883	-2.296	-1.866	-1.544	-1.297	
0.100	-21.510	-14.394	-9.945	-7.092	-5.213	-3.941	-3.057	-2.427	-1.966	-1.621	-1.358	-1.153	
0.150	-11.786	-8.445	-6.216	-4.693	-3.627	-2.864	-2.305	-1.888	-1.571	-1.325	-1.131	-0.975	
0.200	-3.439	-3.216	-2.854	-2.474	-2.122	-1.816	-1.557	-1.341	-1.161	-1.011	-0.887	-0.782	
0.250	2.197	0.487	-0.361	-0.752	-0.905	-0.935	-0.905	-0.848	-0.781	-0.714	-0.650	-0.591	
0.300	4.700	2.364	1.053	0.321	-0.082	-0.298	-0.406	-0.452	-0.464	-0.457	-0.439	-0.417	
0.350	4.532	2.623	1.470	0.769	0.341	0.080	-0.078	-0.172	-0.226	-0.254	-0.267	-0.269	
0.400	2.749	1.830	1.191	0.749	0.445	0.237	0.095	-0.002	-0.067	-0.110	-0.137	-0.154	
0.450	0.564	0.666	0.601	0.481	0.355	0.244	0.152	0.080	0.024	-0.017	-0.048	-0.070	

from (2). The values of  $B$  in Fig. 1(b) cover the usual range for organic molecular crystals at room temperature. Fig. 2 displays  $2s$  density functions of  $(^4S)$  N for various  $r$  and  $B$  values as computed from (2). Fig. 3 shows  $2p$  density functions for the  $(^4S)$  N atom as computed from (3). The functions are normalized to give an integrated density of 2 and 3 electrons in Figs. 2 and 3 respectively.

The most dramatic change in the electron density of the atom is the rapid decrease in density at the time average nuclear position for a small increase in the r.m.s. amplitude of vibration from the at-rest condition. For the  $2s$  case, the trough near the zero density point ( $0\cdot168 \text{ \AA}$ ) is well filled, in the time average picture, for a r.m.s. amplitude of  $0\cdot18 \text{ \AA}$  or more. The  $2p$  density function builds up density at the time-average nuclear position and reaches a maximum at  $B=1\cdot4 \text{ \AA}^2$  ( $\langle u^2 \rangle^{1/2}=0\cdot23 \text{ \AA}$ ). Beyond  $0\cdot4 \text{ \AA}$  from the time-average

nuclear position, both the  $2s$  and  $2p$  density functions are very slightly altered by increasing r.m.s. amplitudes of vibration.

The effect of series termination error for the reconstruction of the total atomic density has been discussed by Atoji (1957), Ibers (1961) and Allmann (1967). It is sufficient here to point out that the contribution from the  $1s$  atomic orbital products is the one most affected by series termination error. For example, at a  $B$  value of  $2\cdot5 \text{ \AA}^2$  the  $1s$  density function for the atoms boron through fluorine cannot be faithfully reconstructed (within  $0\cdot01 \text{ e. \AA}^{-3}$  everywhere) unless the limiting sphere radius is greater than  $1\cdot4 \text{ \AA}^{-1} \sin \theta/\lambda$ . The restrictions for  $2s$  and  $2p$  density functions are much less severe and one may expect a virtual elimination of the series termination error in the valence Fourier difference synthesis, as will be shown below.

Table 3. Partial derivative of the total N atom density with respect to  $B$  divided by the total N density function for various values of  $\sin \theta_{\max}/\lambda$ ,  $B$ , and  $R$

The units of the dependent variables are the same as for Table 1.

$R$	$B$	$(\partial \rho / \partial B) / \rho$												
		Limit 0·65												
		2·50	3·00	3·50	4·00	4·50	5·00	5·50	6·00	6·50	7·00	7·50	8·00	
0	-0·183	-0·177	-0·170	-0·163	-0·157	-0·151	-0·145	-0·140	-0·134	-0·129	-0·124	-0·119		
0·050	-0·183	-0·176	-0·169	-0·163	-0·156	-0·150	-0·144	-0·139	-0·134	-0·128	-0·123	-0·119		
0·100	-0·180	-0·173	-0·166	-0·160	-0·154	-0·148	-0·142	-0·137	-0·131	-0·126	-0·122	-0·117		
0·150	-0·175	-0·168	-0·162	-0·156	-0·150	-0·144	-0·138	-0·133	-0·128	-0·123	-0·118	-0·114		
0·200	-0·168	-0·162	-0·155	-0·149	-0·144	-0·138	-0·133	-0·128	-0·123	-0·118	-0·114	-0·110		
0·250	-0·158	-0·152	-0·146	-0·141	-0·135	-0·130	-0·125	-0·121	-0·116	-0·112	-0·108	-0·104		
0·300	-0·145	-0·140	-0·135	-0·129	-0·125	-0·120	-0·116	-0·112	-0·108	-0·104	-0·100	-0·097		
0·350	-0·128	-0·124	-0·119	-0·115	-0·111	-0·107	-0·104	-0·100	-0·097	-0·094	-0·091	-0·088		
0·400	-0·106	-0·103	-0·100	-0·097	-0·094	-0·092	-0·089	-0·087	-0·085	-0·082	-0·080	-0·078		
0·450	-0·076	-0·076	-0·075	-0·074	-0·074	-0·073	-0·072	-0·071	-0·070	-0·069	-0·068	-0·067		
0·500	-0·036	-0·040	-0·043	-0·046	-0·048	-0·050	-0·051	-0·052	-0·053	-0·053	-0·053	-0·053		
Limit 0·80														
$R$	$B$	1·50	2·00	2·50	3·00	3·50	4·00	4·50	5·00	5·50	6·00	6·50	7·00	
		-0·286	-0·270	-0·254	-0·239	-0·225	-0·211	-0·198	-0·187	-0·176	-0·166	-0·156	-0·148	
		-0·284	-0·267	-0·252	-0·237	-0·223	-0·209	-0·197	-0·185	-0·174	-0·164	-0·155	-0·147	
0·050	-0·277	-0·261	-0·246	-0·231	-0·217	-0·204	-0·192	-0·181	-0·170	-0·160	-0·151	-0·143		
0·100	-0·265	-0·250	-0·235	-0·221	-0·208	-0·195	-0·184	-0·173	-0·163	-0·154	-0·146	-0·138		
0·150	-0·247	-0·233	-0·219	-0·206	-0·194	-0·182	-0·172	-0·162	-0·153	-0·145	-0·137	-0·130		
0·200	-0·221	-0·208	-0·196	-0·185	-0·175	-0·165	-0·156	-0·147	-0·140	-0·133	-0·126	-0·120		
0·250	-0·185	-0·175	-0·166	-0·157	-0·150	-0·142	-0·135	-0·129	-0·123	-0·118	-0·113	-0·108		
0·300	-0·132	-0·129	-0·125	-0·121	-0·118	-0·114	-0·110	-0·107	-0·104	-0·100	-0·097	-0·094		
0·350	-0·056	-0·065	-0·071	-0·075	-0·078	-0·080	-0·080	-0·081	-0·080	-0·080	-0·079	-0·078		
0·400	0·059	0·025	0·001	-0·017	-0·029	-0·039	-0·046	-0·051	-0·054	-0·057	-0·059	-0·060		
0·450	0·237	0·149	0·093	0·054	0·027	0·008	-0·007	-0·018	-0·026	-0·033	-0·037	-0·041		
Limit 1·20														
$R$	$B$	0·50	1·00	1·50	2·00	2·50	3·00	3·50	4·00	4·50	5·00	5·50	6·00	
		-0·686	-0·604	-0·528	-0·459	-0·399	-0·349	-0·307	-0·272	-0·244	-0·220	-0·200	-0·183	
		-0·675	-0·594	-0·518	-0·451	-0·392	-0·343	-0·302	-0·268	-0·240	-0·217	-0·198	-0·181	
0·050	-0·639	-0·560	-0·488	-0·424	-0·370	-0·325	-0·287	-0·256	-0·230	-0·208	-0·190	-0·175		
0·100	-0·569	-0·497	-0·434	-0·379	-0·332	-0·294	-0·262	-0·235	-0·213	-0·194	-0·179	-0·165		
0·150	-0·445	-0·393	-0·348	-0·310	-0·277	-0·250	-0·226	-0·207	-0·190	-0·175	-0·163	-0·152		
0·200	-0·214	-0·224	-0·222	-0·215	-0·204	-0·193	-0·182	-0·171	-0·161	-0·152	-0·143	-0·135		
0·250	0·275	0·057	-0·042	-0·090	-0·115	-0·126	-0·130	-0·130	-0·128	-0·124	-0·120	-0·116		
0·300	1·618	0·512	0·194	0·056	-0·014	-0·052	-0·073	-0·085	-0·091	-0·094	-0·095	-0·094		
0·350	6·948	1·093	0·432	0·195	0·081	0·019	-0·018	-0·041	-0·054	-0·063	-0·069	-0·072		
0·400	6·317	1·169	0·515	0·269	0·144	0·073	0·028	-0·001	-0·020	-0·033	-0·042	-0·049		
0·450	0·465	0·435	0·325	0·226	0·152	0·098	0·059	0·030	0·009	-0·006	-0·018	-0·027		

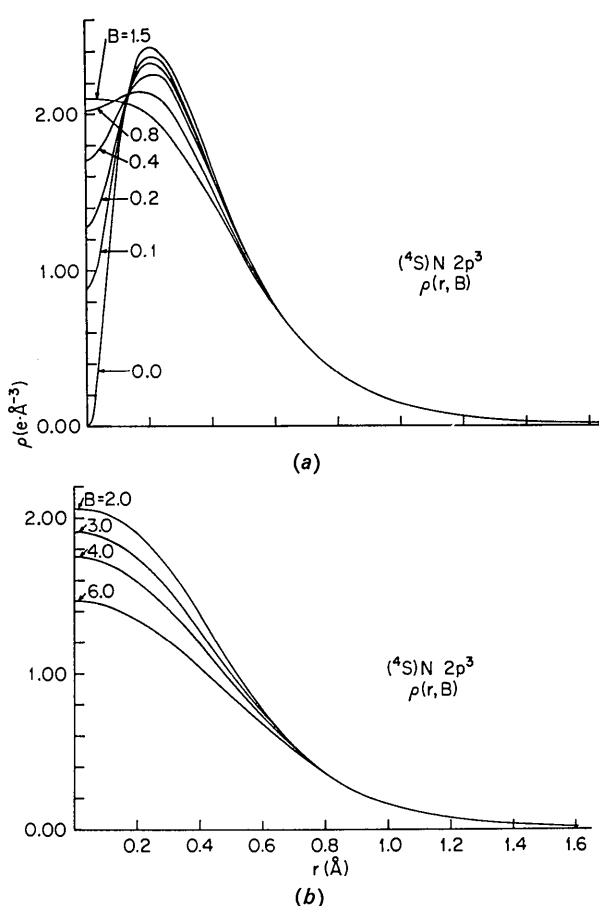


Fig. 3. Vibrational modification of the radial, atomic  $2p$  density piece for  $(^4S)$  N atom. The density functions are normalized as in Fig. 1 to 3 electrons. (a) Low temperature case. (b) Room temperature case.

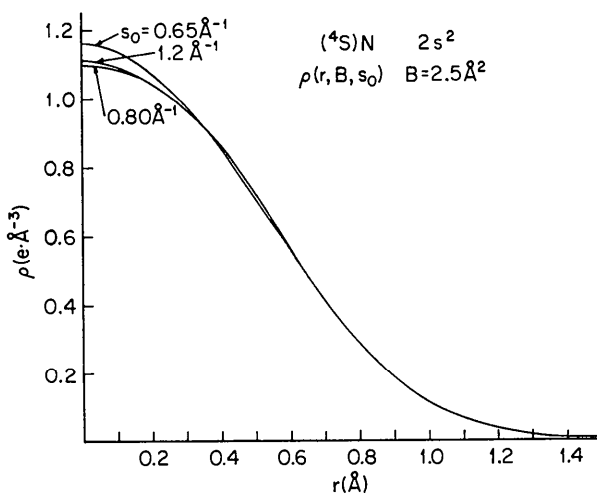


Fig. 4. The effect of series termination on the atomic  $2s$  density for  $(^4S)$  N with a root mean square amplitude of  $0.31\text{\AA}$ . The curve for Fourier coefficients up to  $1.2\text{\AA}^{-1}$  is virtually the same curve for  $s_0 = \infty$ .

The functions  $\partial\varrho_{1s}(r, B, S_0)/\partial B$ ,  $\partial\varrho(r, B, S_0)/\partial B$ , and  $(\partial\varrho/\partial B)/\varrho$  for the N atom density are compiled in Tables 1, 2 and 3 respectively. For the compilation of these tables, the partial derivative of (4) with respect to  $B$  was evaluated. The scattering factors  $f_{at}(S)$  were computed from the Fourier transforms of Clementi's analytical wave functions (Clementi *et al.*, 1962). The derivative function in Table 1 is most useful for assessing errors in valence Fourier difference maps as a result of errors in the thermal parameters. For full difference maps, where the total density of an isolated atom (more appropriately, the incomplete Fourier transform of the isolated atom) is subtracted out, one should use Table 2. The extension of Tables 1 and 2 to other first row atoms (B through F) may be approximately determined by a factor  $(1.14)^{n-1}$ , where  $n$  is the atomic number for the atom of interest.

The partial derivatives in Tables 1 and 2 vary considerably for different values of  $r, B$  and  $S_0$ . One major overall conclusion is that errors at or near the time average position of the nucleus are very large for typical, estimated standard deviations in  $B$  of about  $0.1\text{\AA}^2$ . For example, for an N atom with a  $B$  of  $3.0\text{\AA}^2$ , and the limit of data at  $0.65\text{\AA}^{-1}$  (the Cu  $K\alpha$  limit), the error in the density at the nucleus is  $\pm 0.2\text{ e.\AA}^{-3}$ . An error larger than  $\pm 0.1\text{ e.\AA}^{-3}$ , at this resolution, persists out to  $0.3\text{\AA}$ . For data out to  $0.8\text{\AA}^{-1}$  in  $\sin\theta/\lambda$ , the error in  $\varrho_v$  is  $\pm 0.47\text{ e.\AA}^{-3}$  at the nucleus but falls off more rapidly than for the lesser resolution in Cu  $K\alpha$  data. Nonetheless, an error greater than  $\pm 0.1\text{ e.\AA}^{-3}$  again persists out to  $0.3\text{\AA}$ . We assumed here that the error in  $B$  is  $\pm 0.1\text{\AA}^2$ . If we contemplate low temperature studies and consider lower  $B$  values, we see that for  $B = 1.5\text{\AA}^2$ , the error at a nitrogen nucleus is  $\pm 0.55\text{ e.\AA}^{-3}$  for  $\Delta B = \pm 0.1\text{\AA}^2$  and for a cutoff of  $0.8\text{\AA}^{-1}$ . For a cutoff at  $1.2\text{\AA}^{-1}$ , the error in  $\varrho_v$  is  $\pm 1.7\text{ e.\AA}^{-3}$ . This falls off rapidly within a sphere of  $0.25\text{\AA}$ , but becomes  $\mp 0.1\text{ e.\AA}^{-3}$  in a shell from  $0.35\text{\AA}$  to  $0.45\text{\AA}$ .

The values tabulated in Table 3 are an estimate of the relative error in an electron density map of a nitrogen atom constructed by Fourier synthesis. Results for other first row atoms agree with those given in Table 3 to within 5% except for low  $B$  values ( $0.5$ – $1.0\text{\AA}^2$ ) and high resolution ( $\sin\theta_{\max}/\lambda \geq 1.00\text{\AA}^{-2}$ ) where quantum effects are appreciable. For an error of  $0.1\text{\AA}^2$  in  $B$ , the relative error near the time-average nuclear position is about 3% in the room temperature case. For lower  $B$  values and larger resolution ( $\sin\theta_{\max}/\lambda = 1.2\text{\AA}^{-1}$ ), the relative error becomes larger. At distances greater than  $0.4\text{\AA}$  from the nuclear position, the relative error falls below 1%. If  $\bar{\rho}_o$  is larger than  $\bar{\rho}_c$  in the bonding region, which is usually true, the relative error would be still smaller than the estimate from Table 3.

We assume that the valence density is built up principally by  $2s$  and  $2p$  type shape functions. The radial behavior of these functions provide us with the principal criterion as to the appropriate limiting sphere

in reciprocal space. The angular dependence is a detailed property of the particular molecular crystal and is presumably contained in the experimental structure factors. In the absence of large systematic errors in the observed structure factors we need only consider series termination errors in the reconstruction of  $2s$  and  $2p$  density functions.

Fig. 4 is a plot of  $2s$  density, calculated from the incomplete Fourier transform (4), for constant Debye-Waller factor,  $B=2.5 \text{ \AA}^2$ . The curve for  $\rho(r, 2.5, \infty)$  is virtually the same as for  $S_0=1.2 \text{ \AA}^{-1}$ . Note that for low resolution ( $S_0 \leq 0.65 \text{ \AA}^{-1}$ ), the time-average density at the nucleus is larger than the true result, whereas for higher resolution ( $S_0=0.8 \text{ \AA}^{-1}$ ), the density is smaller. For the  $2p$  density case, displayed in Fig. 5, the series-terminated density is always larger at the nucleus than the true result. Note that the  $2p$  density for  $S_0=0.65 \text{ \AA}^{-1}$  and for  $S_0=0.8 \text{ \AA}^{-1}$  are virtually identical. About  $0.25 \text{ \AA}$  from the time average nuclear position both the  $2s$  and  $2p$  densities are accurately reconstructed ( $< \pm 0.01 \text{ e. \AA}^{-3}$ ) within a sphere  $1.2 \text{ \AA}^{-1}$  in  $\sin \theta/\lambda$ . This holds down to  $B$  values of  $1.0 \text{ \AA}^2$ . A sphere of  $0.8 \text{ \AA}^{-1}$  is adequate for reconstruction of  $2s$  and  $2p$  density functions at  $B \geq 2.5 \text{ \AA}^2$  – a typical room temperature case. The major qualitative result is that a

sphere of  $0.8 \text{ \AA}^{-1}$  or larger ought to be sufficient for synthesis of valence density maps. For the low temperature case, an effective sphere of the data ought to be extended to  $1.2 \text{ \AA}^{-1}$  in  $\sin \theta/\lambda$ .

It should be noted here that scattering from bonded electrons, that is, from  $2s$  and  $2p$  density functions, for the first row atoms becomes rather small at  $\sin \theta/\lambda > 0.5 \text{ \AA}^{-1}$  and the contribution to any one structure factor is about 3% to 5% of the total atomic scattering factor at high  $\sin \theta/\lambda (> 0.7 \text{ \AA}^{-1})$  values. Nonetheless, in a Fourier synthesis, the radial distribution in reciprocal space for the  $2s$  and  $2p$  scattering factors ( $f_v$ 's) reveals that the contribution to the electron density does not become marginal ( $< 0.01 \text{ e. \AA}^{-3}$ ) until the cutoff is about  $0.8 \text{ \AA}^{-1}$ . The reason for this effect is that the contribution to the Fourier density from each  $f_v$  goes up as  $(\sin \theta/\lambda)^2$  while the resolution is increased. A nice illustration of the high order effect has been given by O'Connell, Rae & Maslen (1966).

### Conclusion

We have developed accurate formulae for the convolution of one-electron density functions onto a Gaussian distribution function for the nucleus. These time-aver-

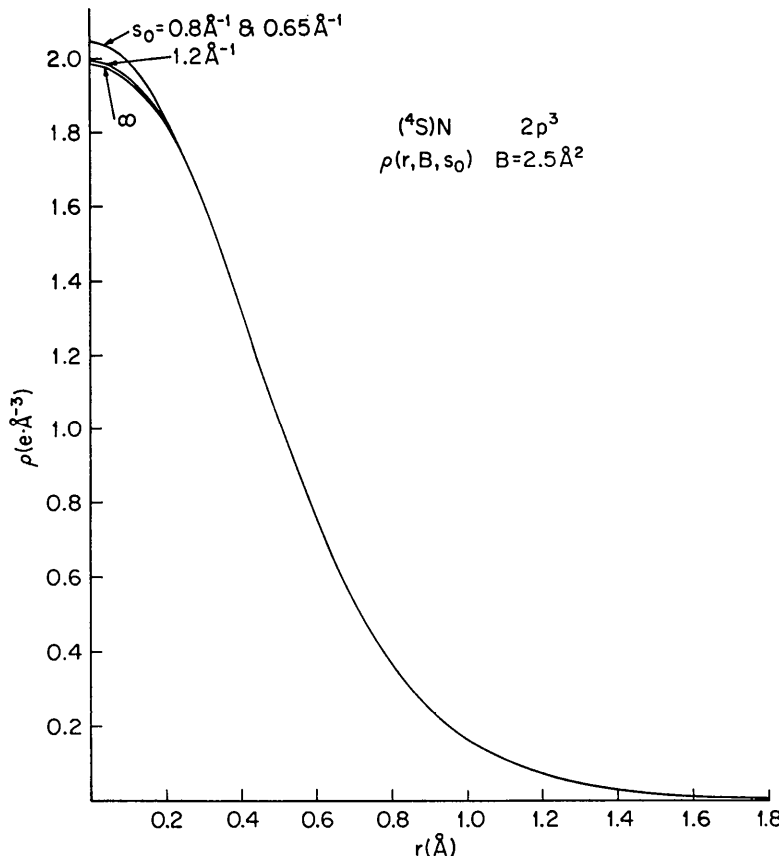


Fig. 5. The effect of series termination on the radial atomic  $2p$  density function for  $(^4S) N$  with a root mean square amplitude of  $0.31 \text{ \AA}$ .

age electron distribution functions are considerably modified compared with the atom at rest. The functions  $\partial\varrho(r, B, S_0)/\partial B$ , indicate that, with present day precision of thermal parameters, Fourier difference maps are uninterpretable within 0.3 Å of the time-average nuclear position. If we assume that the lower limit for estimated standard deviations in the density as a result of errors in observed structure factors is 0.01 e.Å<sup>-3</sup>, then beyond 0.4 Å from the time-average nuclear position, the residual density does not suffer significant bias due to thermal parameter errors. The tabulations of the partial derivatives in Tables 1 and 2 are applicable to error analysis in real X-ray diffraction density maps provided a high proportion of the reflections within the limiting sphere are observed. For the case of anisotropic thermal motion, it is sufficient at small  $r$  to take

$$B = (B_1 B_2 B_3)^{1/3},$$

where the  $B_j$  are principal values. Beyond ~0.25 Å, one should use (5) and take partial derivatives with respect to the  $B_j$ 's.

Valence Fourier difference maps cannot easily be used for quantitative analysis of valence structure. The bias from rather imprecise thermal parameters in an  $F_c$  calculation yields a very large density error (>0.1 e.Å<sup>-3</sup>) near the nuclear positions. Valence electron densities 0.5 Å beyond the nuclei ought to be free from parametric errors in the  $F_c$  calculation compared with errors in  $F_o$ . One should go beyond the limit of Cu  $K\alpha$  radiation (0.648 Å<sup>-1</sup>) to ~0.8 Å<sup>-1</sup> to get a valence map free from series termination error. For low temperature work, the data should be extended to ~1.2 Å<sup>-1</sup> in  $\sin \theta/\lambda$ .

The error in the residual electron density as a result of the error in a scale factor is simply,

$$\sigma(\varrho)/\varrho = \sigma(k)/k,$$

where  $k$  is the scale factor. For most accurate structures of organic molecular crystals,  $\sigma(k)/k$  is less than 0.01. For  $\sigma(B)=0.1$  Å<sup>2</sup>, we saw that for first row atoms,  $\sigma(\varrho)/\varrho$  as computed from Table 3, is 0.04 to 0.02 near the time-average nuclear position. In the absence of large systematic errors in the low-order structure factors, which can lead to a large error in  $k$ , the bias from thermal parameter errors is more severe than it is from a scale factor error. In a bonding region, about 0.4 Å from the nucleus, it can be expected that both sources of error have comparable variances.

I gratefully thank Professor John Pople for useful discussions on this work. The attentive help by Dr E. N. Maslen and Professor D. P. Shoemaker in the revision of this manuscript is much appreciated. This work has been supported by NIH General Research Grant FR558001-5.

#### References

- ALLMANN, R. (1967). *Acta Cryst.* **22**, 434.
- ATOJI, M. (1957). *Acta Cryst.* **10**, 291.
- BLOCH, F. (1932). *Z. Phys.* **74**, 295.
- CLEMENTI, E., ROOTHAAN, C. C. J. & YOSHIMINE, M. (1962). *Phys. Rev.* **127**, 1618.
- DAWSON, D. (1964). *Acta Cryst.* **17**, 997.
- HIGGS, P. W. (1953). *Acta Cryst.* **6**, 232.
- HUZINAGA, S. (1965). *J. Chem. Phys.* **42**, 1293.
- IBERS, J. (1961). *Acta Cryst.* **14**, 538.
- O'CONNELL, A. M., RAE, A. I. & MASLEN, E. N. (1966). *Acta Cryst.* **21**, 208.
- ZACHARIASEN, W. H. (1967). *Phys. Rev. Letters*, **18**, 195; *Acta Cryst.* **23**, 558.

*Acta Cryst.* (1968). A **24**, 505

## Détermination du Nombre de Faisceaux dans le Calcul de l'Intensité Intégrée d'une Tache de Diffraction Électronique

PAR P. HAYMANN

Faculté des Sciences, 76 Mont Saint-Aignan, France

(Reçu le 28 septembre 1967, revu le 8 février 1968)

It is shown to what extent it is possible to calculate the number of beams which interfere in the case of systematic interactions of a reciprocal spot  $\mathbf{h}$ . In the case in which it is supposed that the interference between these various beams (belonging to the reciprocal line which produces the systematic interaction) and the diffracted beam  $\mathbf{h}$  can be treated in the two-beam approximation and cannot occur if the relative proportion of the wave amplitudes is below a definite value, this criterion gives a simple method of handling a number of diffracted beams whatever the angle of incidence of the electron beam may be. Results of calculations are given for different metals and different conditions of excitation.

Les théories matricielles (Fujimoto, 1959; Sturkey, 1962; Niehrs & Wagner, 1955; Tournarie, 1960) de la diffraction électronique donnent les expressions de l'intensité d'une tache pour une direction bien déter-

minée du vecteur d'onde incident. Elles permettent également de fixer le nombre de faisceaux et donc le rang des matrices au moyen de différentes méthodes. Celles-ci cependant s'avèrent d'emploi difficile lorsqu'il